

Article

Future Changes in Precipitation and Drought Characteristics over Bangladesh under CMIP5 Climatological Projections

Mohammad Kamruzzaman ^{1,2} , Min-Won Jang ¹ , Jaepil Cho ³ and Syewoon Hwang ^{1,*}

¹ Department of Agricultural Engineering, Institute of Agriculture and Life Science, Gyeongsang National University, 52828, 501, Jinju-daero, 13557 Jinju, Gyeongsangnam, Korea; milonbrri@gmail.com (M.K.); mwjang@gnu.ac.kr (M.-W.J.)

² Bangladesh Rice Research Institute, Gazipur 1701, Bangladesh

³ Research Department, APEC Climate Center, Busan 48058, Korea; jpcho89@gmail.com

* Correspondence: swhwang@gnu.ac.kr; Tel.: +82-55-772-1934

Received: 18 September 2019; Accepted: 22 October 2019; Published: 24 October 2019



Abstract: The impacts of climate change on precipitation and drought characteristics over Bangladesh were examined by using the daily precipitation outputs from 29 bias-corrected general circulation models (GCMs) under the representative concentration pathway (RCP) 4.5 and 8.5 scenarios. A precipitation-based drought estimator, namely, the Effective Drought Index (EDI), was applied to quantify the characteristics of drought events in terms of the severity and duration. The changes in drought characteristics were assessed for the beginning (2010–2039), middle (2040–2069), and end of this century (2070–2099) relative to the 1976–2005 baseline. The GCMs were limited in regard to forecasting the occurrence of future extreme droughts. Overall, the findings showed that the annual precipitation will increase in the 21st century over Bangladesh; the increasing rate was comparatively higher under the RCP8.5 scenario. The highest increase in rainfall is expected to happen over the drought-prone northern region. The general trends of drought frequency, duration, and intensity are likely to decrease in the 21st century over Bangladesh under both RCP scenarios, except for the maximum drought intensity during the beginning of the century, which is projected to increase over the country. The extreme and medium-term drought events did not show any significant changes in the future under both scenarios except for the medium-term droughts, which decreased by 55% compared to the base period during the 2070s under RCP8.5. However, extreme drought days will likely increase in most of the cropping seasons for the different future periods under both scenarios. The spatial distribution of changes in drought characteristics indicates that the drought-vulnerable areas are expected to shift from the northwestern region to the central and the southern region in the future under both scenarios due to the effects of climate change.

Keywords: Effective Drought Index (EDI); meteorological drought; climate change; GCMs under RCP scenarios; future drought projections; Bangladesh

1. Introduction

Nowadays, climate change is regarded as a major global issue, and it poses significant challenges to human existence and socio-economic development, particularly in Bangladesh. The dominant features of climate change in Bangladesh detected in the late 19th century include the significant increases in temperature and monsoon and post-monsoon precipitation due to global warming. However, a decreasing trend of precipitation was observed in the winter season [1]. The overall increasing rate of warming in Bangladesh is higher than the present increasing rate of global warming, and this trend is expected to continue over the 21st century [2–4]. Notably, Bangladesh has been suffering from

frequent natural disasters. Among the most expensive natural disasters, drought is a chronic natural disaster that can have severe and long-lasting impacts on water resources, agriculture, ecosystems, and human societies [5]. The impact of drought events is often worst in developing countries because their economies are driven mainly by agricultural products that are adversely affected by meteorological droughts [6]. Drought may generally be defined as a scarcity of water in a region over a prolonged period of time triggered by a lack of rainfall. Presently, great effort needs to be expended on researching future changes in rainfall patterns, which are the major causes of drought in Bangladesh and can lead to adverse changes in economic and social development. The effects of gradual climate changes and extreme weather events may negatively impact overall socio-economic development in many regions, and therefore, the scientific community and policymakers need more information about the probability of future occurrences of such events [7,8].

The Coupled Model Intercomparison Project (CMIPs) has made available general circulation model (GCM) outputs for the Programme for Climate Model Diagnosis and Intercomparison (PCMDI), and these products are available for research. The climate model outputs from Phase 3 of the CMIP (CMIP3) were broadly used in the Intergovernmental Panel on Climate Change (IPCC) 4th Assessment Report (AR4) [9]. Recently, climate models from Phase 5 of the CMIP (CMIP5) along with greenhouse gas concentration scenarios termed as representative concentration pathways (RCPs) were adopted by the IPCC for its 5th Assessment Report (AR5) [10]. The models from CMIP5 joined with the RCP scenarios have delivered more precise representations of climate outputs than the CMIP3 model results because corrections were made in regard to some key assumptions of climate that were overlooked previously by the model developers [11]. Sperber et al. [12] demonstrated that the CMIP5 models are more competent for capturing numerous features of the Asian monsoon climate compare to the CMIP3 models. Therefore, it is of supreme importance to assess future changes in climatological drought by using the precipitation data from the new sets of CMIP5 GCM projections.

Presently, GCMs are the principal tools for predicting and projecting future climate changes. However, most such global climate models are typically run at coarse resolutions, e.g., more than hundreds of kilometers. Therefore, the GCM outputs are inherently unable to represent regional or local climate features and dynamics at the necessary spatial resolutions for detailed analyses [13]. To overcome this problem, downscale techniques have been developed to obtain local climate change information at the desired scale from coarser-resolution GCM outputs [14,15]. Dynamic downscaling data have been recognized to be more representative of fine-scale physical processes than statistical downscaling data; however, the former technique requires more expensive computing resources than the latter technique [16–18]. A large number of simulations with multiple GCM configurations and emissions scenarios can be computed efficiently by using a statistical approach, and such an approach is well accepted in the scientific community; these types of data are widely used in downscaling climate projections. Thus, projections from multiple GCMs from CMIP5 have been used in this study.

In parallel, climate change impact assessments at the regional scale rarely use the raw GCM outputs because climate model data suffer from systematic biases due to the uncertainty in the parameterization of unsolved processes [19]. Therefore, bias-corrected GCM outputs are essential for regional climate impact studies and vulnerability assessments. A vast number of bias correction procedures are in use, such as the monthly mean correction [20], delta change [21], and quantile mapping [22] techniques. The quantile mapping methods are considered to be the most accurate methods in terms of precipitation [23] among all of the other methods. Therefore, a quantile based bias correction approach was used to adjust for the model biases in this study.

One way of assessing the changes in future drought characteristics is to use climate projections from a couple of GCM simulations under different greenhouse gas emission scenarios [24]. According to Coelho and Goddard [25], future changes in precipitation patterns may aggravate drought risk in highly vulnerable tropical areas. In several areas, climate change is expected to primarily affect precipitation, and thus, it is likely to affect the frequency and severity of metrological droughts. A remarkable number of studies have assessed the future drought risks on global and regional scales by using multiple

climate model scenarios [26–29]. For instance, Chen et al. [30] investigated the future change in the drought pattern over the 21st century in China by using global climate models and regional climate models (RCMs) under the SRES (Special Report on Emissions Scenarios) A1B scenario, and the findings indicated that droughts will become less frequent in most areas of China. Conversely, Wang et al. [31] examined future drought in China by using CMIP5 model outputs under the RCP4.5 and RCP8.5 scenarios and revealed that extreme drought events would increase in the future. This discrepancy may have been due to the limitations of drought indices and the lack of realistic climate information. Importantly, the future drought outlook may depend on the indicators used in drought calculations along with realistic climate data. The selection of appropriate drought indices is therefore vital for understanding the future drought characteristics and for planning a drought mitigation strategy for a region [32]. Hence, it is necessary to predict future drought characteristics on a local scale by using realistic climate information and locally applicable and appropriate drought indices.

In the past few years, several studies have projected the average temperatures and annual rainfall for Bangladesh in the future [33–35]. For instance, Rahman et al. [34] estimated the annual rainfall by using version 3 of an RCM (RegCM3), and the findings indicated that a 50% decrease in rainfall will occur by 2060. Nowreen et al. [33] found that the amount of total rainfall is likely to increase in the future based on simulations with a 17-member ensemble-driven by the Hadley Centre Coupled Model (HadCM3). A number of studies have suggested that the overall monsoon rainfall will increase and post-monsoon rainfall will decrease in the future throughout most parts of the country [34,35]. Notably, very few studies have been done concerning future drought projections [35,36]. Islam et al. [36] evaluated the drought hazards at current and future climate change conditions in the western region of Bangladesh by using simulated climate data from the outputs of three global climate models for the period between 2041 and 2070. Hasan et al. [35] estimated the future drought conditions by using 25 km high resolution downscaled and projected climate data generated from the RCM known as PRECIS for a continuous period of 1971–2100. The results revealed that droughts will generally decrease in future years but there will be a comparative higher frequency of droughts in the mid 21st century. However, all of these studies used the climate model output from CMIP3 and were driven by the previous IPCC AR4 scenarios.

Recently, Hasan et al. [37] projected the future climate and associated extremes while considering the new RCP4.5 and RCP8.5 scenarios by using RCM results driven by the GCMs over Bangladesh within the new CMIP5. The study revealed that overall precipitation and temperature trends are likely to increase in the future over this region. However, drought characteristics were not evaluated by using these outputs. Mortuza et al. [38] projected only the future drought frequency from 2020 to 2100 by using bias-corrected four GCM (CMIP5) model outputs under the RCP4.5 and RCP8.5 scenarios and showed that the drought frequency will decrease in the future (2020–2100) compared to the past (1961–2010). They also pointed out that more frequent and severe droughts will occur on the west side of the country. However, a complete assessment of future changes in drought characteristics in terms of the frequency, duration, and intensity of meteorological drought events and seasonal drought days mainly based on CMIP5 multimodel simulated data still has not been performed to understand the future conditions of droughts in Bangladesh, and this was the prime motivation for this study. The downscaling techniques of spatial disaggregation were utilized in this study to provide finer-resolution climate projections.

Over the years, a good number of drought indices (DIs) have been proposed and developed to identify the spatiotemporal patterns of droughts and quantify their intensity. The maximum number of drought indices is region-specific, as indices are limited in terms of their applications to different climatic conditions due to the inherent complexity of drought phenomena. In Bangladesh, most of the studies have measured drought severity by using the Standardized Precipitation Index (SPI; [39]), while very few research studies have used other DIs. The SPI is calculated based on the averaged monthly precipitation for a certain period. Therefore, the time steps involved in the SPI tend to produce several different values for the same period. Additionally, the SPI does not take into account

the water resources generated by rainfall that may have already been lost due to outflow as well as the effect of evaporation. Moreover, the SPI tends to assign equal weight to temporally different precipitation events, thereby resulting in inaccuracies in predictions of the drought severity [40]. Byun and Wilhite [41] developed a new series of indices to overcome these limitations. Specifically, they used a new concept of effective precipitation (EP), in which the EP represents the summed value of all daily precipitation with a time-dependent reduction function. The EDI was found to be more responsive to drought conditions compared with other drought indices, and it could capture the real essence of the meteorological drought situation in the study area [42–45]. In particular, Kamruzzaman et al. [46] empirically demonstrated the superiority of the EDI over the SPI when monitoring both long-term and short-term droughts in Bangladesh. Thus, the EDI was employed in this study to interpret the changes in drought patterns to gain knowledge about the potential future changes in drought over Bangladesh.

With the aim of investigating the future changes in precipitation and meteorological drought characteristics over Bangladesh, the drought characteristics were assessed by using the EDI and the bias-corrected CMIP5 GCM precipitation data under the RCP4.5 and RCP8.5 scenarios from 2010 to 2100 were used in this study. Twenty-nine different GCMs and corresponding Multi-Model Ensemble (MME) means were evaluated to assess the performance of the models in reproducing the observed drought characteristics during the historical period and for deriving future changes in drought characteristics in terms of the frequency, duration, and severity. The changes were evaluated in three future time ranges, namely, the 2010s (2010–2039), 2040s (2040–2069), and 2070s (2070–2099), and data were compared to the baseline period (1976–2005).

2. Materials and Methods

2.1. Study Area and Observation Data

The study area covers Bangladesh, which is situated in latitudes between 20°34' and 26°38' north and longitudes between 88°01' and 92°41' east in South Asia; this region is bordered by India on three sides (i.e., west, north, and northeast), and it is bordered by Myanmar to the southeast. The southern border is demarcated by the Bay of Bengal with a long coastline. Although elevations up to 105 m above sea level occur in the northern part of the country, most of the elevations are less than 10 m above sea level; heights decrease in the coastal south (Figure 1). A predominance of agricultural lands is evident, and such lands comprise three-fourths of the total geographical area followed by forests, including orchards, as shown in Figure 2. Bangladesh is one of the most vulnerable nations to the increasing effects of global climate change. Presently, this country is regularly affected by natural disasters such as floods, tornadoes, droughts, and tidal bores. It has experienced drought conditions recurrently over the past several years; on average, these events have occurred once in 2.5 years [47] and have mainly affected agricultural lands, with huge losses in food grains [48,49]. While drought is a periodic occurrence in many parts of Bangladesh, the northwestern part of the country is the most susceptible to drought due to the high variability of rainfall [50]. During 2006, the average crop production was decreased by 25–30% due to the effects of drought in the northwestern part of Bangladesh [51]. This area is comparatively dry in relation to other areas of the country, as it receives much lower rainfall [52]. Additionally, this area contains sandy soils that have a low moisture retention capacity and a high infiltration rate [53]. Therefore, drought happens in this region regularly.

The climate of Bangladesh is characterized by moderately warm temperatures, high humidity, and subtropical monsoons with wide seasonal variations in rainfall. The following four meteorological seasons are generally recognized: a hot, humid pre-monsoon period (March to May); a humid, warm, and rainy monsoon period (June to September); a post-monsoon period (October to November); and a dry winter (December to February). Moreover, the cropping season in Bangladesh is categorized into Pre-Kharif (March–June), Kharif (July–October), and Rabi (November–February). The mean annual temperature within the country is about 25 °C. The temperature varies from month to month.

In general, the mean temperature across the country usually ranges between 11 °C and 29 °C and between 21 °C and 34 °C during the summer months. April is the warmest month in most parts of the country [54]. The annual rainfall in the region varies from 1536 mm to 4124 mm during 1976 and 2005, and the 30-year averaged annual rainfall was 2410 mm. (Table 1).

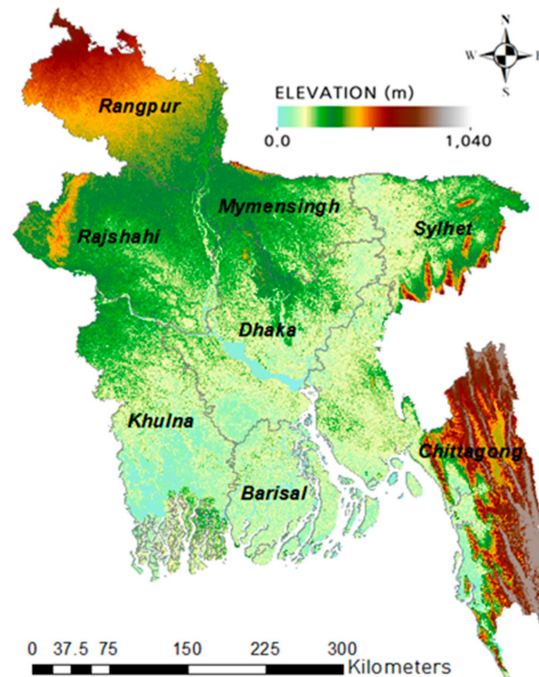


Figure 1. The elevation map of Bangladesh (data source: <https://SRTM.csi.cgiar.org>).

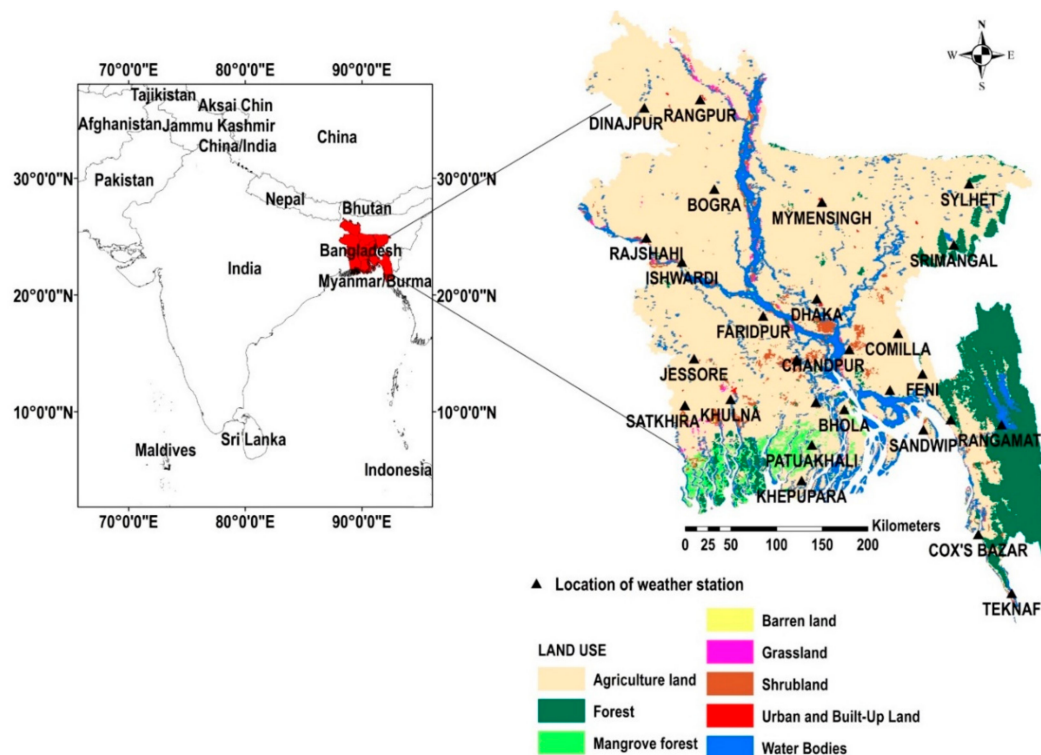


Figure 2. Location of meteorological stations and land use map of the study area.

Table 1. Mean monthly and annual rainfall at various stations in Bangladesh.

Station Name	Data Period	Location		Mean Monthly Rainfall of Multiple Stations During 1976–2005 (mm)												Annual Avg. Precip. (mm)
		Lon.	Lat.	Jan	Feb	Mar	Apr	May	Jun	Jul	Aug	Sep	Oct	Nov	Dec	
Rangpur	1954 to present	89.23	25.73	8	11	25	117	274	453	498	356	383	176	8	9	2318
Dinaipur	1948 to present	88.68	25.65	10	11	14	76	222	358	471	373	370	160	9	10	2082
Bogra	1948 to present	89.37	24.85	8	13	21	79	209	320	402	293	309	152	12	11	1828
Rajshahi	1964 to present	88.70	24.37	10	16	25	65	140	261	327	255	285	127	14	11	1536
Ishwardi	1961 to present	89.05	24.13	6	21	33	86	194	292	326	230	288	117	16	9	1616
Jessore	1948 to present	89.17	23.18	14	26	46	77	176	318	316	274	269	138	29	13	1695
Khulna	1948 to present	89.53	22.78	12	39	53	84	193	355	304	329	251	131	37	8	1795
Shatkhira	1948 to present	89.08	22.72	13	39	42	90	159	295	335	296	280	127	33	9	1717
Barishal	1949 to present	90.37	22.75	10	25	55	119	212	418	419	362	282	178	46	8	2132
Patuakhali	1973 to present	90.33	22.33	8	22	43	115	238	535	540	450	342	185	53	6	2536
Khepupara	1974 to present	90.23	21.98	9	24	49	97	259	513	606	490	369	243	55	8	2721
Bhola	1966 to present	90.65	22.68	10	30	53	131	265	471	447	388	291	172	43	7	2308
Maizdi Court	1951 to present	91.10	22.87	10	27	76	154	335	574	750	631	384	181	44	7	3172
Swandip	1966 to present	91.43	22.48	9	22	68	146	349	699	860	621	436	256	50	9	3526
Dhaka	1953 to present	90.38	23.77	7	22	69	146	318	346	359	298	326	183	29	12	2115
Mymensingh	1948 to present	90.43	24.72	7	22	38	145	359	395	453	326	322	216	18	10	2309
Hatiya	1966 to present	91.10	22.43	4	14	42	116	237	541	557	484	322	193	36	12	2559
Chandpur	1964 to present	90.70	23.27	6	20	61	139	247	341	375	326	259	138	39	7	1956
Comilla	1964 to present	91.18	23.43	7	24	70	149	322	359	411	318	250	154	34	10	2108
Feni	1973 to present	91.42	23.03	6	28	69	180	369	535	652	496	330	181	45	9	2900
Sylhet	1956 to present	91.88	24.9	7	34	149	367	571	769	833	602	529	222	28	13	4124
Srimangal	1948 to present	91.73	24.3	5	30	89	221	445	442	371	336	296	163	32	15	2445
Chittagong	1949 to present	91.81	22.35	4	23	50	128	292	560	645	486	227	179	60	13	2669
Rangamati	1957 to present	92.20	22.53	5	23	62	139	333	504	575	442	294	154	57	13	2601
Cox's Bazar	1948 to present	91.97	21.45	5	18	32	117	301	812	869	668	357	198	95	14	3486
Mean				8	23	53	131	281	459	508	405	322	173	37	10	2410
±				±	±	±	±	±	±	±	±	±	±	±	±	±
STDV				3	8	27	61	96	148	176	126	66	36	20	3	649

The Bangladesh Meteorological Department (BMD) operates 35 weather stations throughout the country. However, only 25 stations have continuous rainfall records for more than 30 years from 1976 to 2005 (Figure 2). In this study, the daily time series rainfall data were used to evaluate the GCM data for the same period. When working with observation data, missing data are common. Here, there were some missing data in the dataset, but the amount was <2%. The average values of the same date from neighboring stations were used in place of the missing data.

2.2. EDI Calculation

In this study, EDI was used to characterize droughts in terms of the frequency, duration, intensity, and seasonal drought days. The estimation of drought features in this method is the use of daily precipitation. The EDI calculation process was carried out according to the following equations:

$$EP_i = \sum_{n=1}^i \left[\left(\sum_{m=1}^n P_m / n \right) \right] \quad (1)$$

$$DEP = EP - ME \quad (2)$$

$$EDI = DEP / ST(DEP) \quad (3)$$

In Equation (1), EP is the daily cumulative effective precipitation, P_m is the precipitation of $m - 1$ days ago, n is the duration of the preceding period, and i is the duration over which precipitation is summed. For example, if i is 4, then the daily EP is $P_1 + \frac{P_1+P_2}{2} + \frac{P_1+P_2+P_3}{3} + \frac{P_1+P_2+P_3+P_4}{4}$. In this study, i was set to 365 days.

Secondly, the mean EP (MEP) is computed for each calendar day, i.e., from 1 to 365, and then the average of the analyzed 30-year period. The MEP is computed with the results from Equation (1). For instance, the MEP of the 1st day of January is the mean of 30 values for the 1st day of January composed over 30 years.

The third step is to calculate the deviation of the EP (DEP) from the MEP (Equation (2)). The DEP indicates the deficiency (negative DEP) or surplus (positive DEP) of water resources for a particular day. If the dry period is longer than 365 days, i in Equation (1) increases by the number of dry days.

For instance, if the negative *DEP* value continues for 2 days, *i* is set to be 367 and Equations (1)–(3) are again calculated.

Finally, the standardized value of *DEP* is calculated, where *ST (DEP)* denotes the standard deviation of each day's *DEP*. The EDI is calculated then by using Equation (3). Originally, the EDI was proposed for monitoring the drought conditions at a daily time step. Then, it was extended for monthly drought monitoring [45,55,56]. In this study, the daily EDI was used for drought calculations.

2.3. Definitions of Drought Characteristics

The EDI value illuminates the characteristics of drought events researched in this study, as shown in Figure 3. A meteorological drought event was considered to have occurred when the EDI values were less than -1 , as shown in Figure 3. The drought start date was considered to be the day in which the EDI first indicated that the value of EDI was -1.0 or below, and the end date was considered to be the day when the EDI regained the value of -1.0 and above. Drought durations are the periods between the start and the end date, as shown in Figure 3. The drought severity is the cumulative deficit below the -1.0 level for the duration of a drought event, as shown in Figure 3, and the maximum intensity of a drought is the value of the minimum EDI at each event.

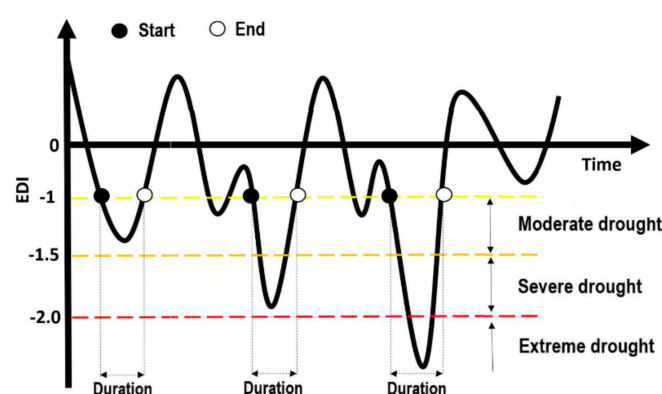


Figure 3. Schematic concept of the drought characteristics (severity, duration) evaluated with the EDI time series.

In this study, the classification level of dryness follows the EDI classification proposed by Kim and Byun [57], as shown in Figure 3, and drought events were also categorized based on the drought duration as shown in Table 2.

Table 2. Drought classification based on the drought duration.

Duration (Days)	Category
Less than or equal to 30	Very short-term
31 to 90	Short-term
91 to 180	Medium-term
Greater than 180	Long-term

The inverse distance weight (IDW) algorithm was used to expand the data to the entire study area spatially. Twenty-five (25) weather station location points of the BMD were considered for spatial mapping of the change in drought characteristics as well as precipitation.

In this study, the following different parameters were used for drought characterization: (a) frequency—number of drought events according to the severity and duration over the period of interest, (b) duration—average duration of all drought events over the period of interest, (c) intensity—extreme intensity (minimum value of EDI) among all of the drought events over the period of interest, and (d) seasonal drought days—number of drought days in each category in different cropping seasons over the period of interest.

2.4. CMIP5 GCM Projections

The CMIP5 projection data, including precipitation for the two RCP scenarios (RCP4.5 and RCP8.5), were acquired from the outputs of 29 CMIP5 GCM models. The GCM models used in this study are described in Table 3.

Table 3. Summary of 29 climate models from CMIP5 used in this study.

Model Name	Modeling Center	Resolution (Lon × Lat)
bcc-csm1-1	Beijing Climate Center, China Meteorological Administration, China	$2.81^{\circ} \times 2.79^{\circ}$
bcc-csm1-1-m		$1.13^{\circ} \times 1.12^{\circ}$
CanESM2	Canadian Centre for Climate Modelling and Analysis, Canada	$2.81^{\circ} \times 2.79^{\circ}$
CCSM4	National Center for Atmospheric Research, USA	$1.25^{\circ} \times 0.94^{\circ}$
CESM1-BGC	National Science Foundation, Department of Energy, National Center for Atmospheric Research, USA	$1.25^{\circ} \times 0.94^{\circ}$
CESM1-CAM5		
CMCC-CM	Centro Euro-Mediterraneo sui Cambiamenti Climatici, Italy	$0.75^{\circ} \times 0.75^{\circ}$
CMCC-CMS		$1.88^{\circ} \times 1.86^{\circ}$
CNRM-CM5	Centre National de Recherches Meteorologiques/Centre Europeen de Recherche et Formation Avancees en Calcul Scientifique, France	$1.41^{\circ} \times 1.40^{\circ}$
CSIRO-Mk3-6-0	Commonwealth Scientific and Industrial Research Organisation in collaboration with the Queensland Climate Change Centre of Excellence, Australia	$1.88^{\circ} \times 1.86^{\circ}$
FGOALS-g2	Institute of Atmospheric Physics, Chinese Academy of Sciences; and CESS, Tsinghua University, China	$2.81^{\circ} \times 3.05^{\circ}$
FGOALS-s2	Institute of Atmospheric Physics, Chinese Academy of Sciences, China	$2.81^{\circ} \times 1.66^{\circ}$
GFDL-CM3	Geophysical Fluid Dynamics Laboratory, USA	$2.50^{\circ} \times 2.00^{\circ}$
GFDL-ESM2G		
GFDL-ESM2M		
HadGEM2-AO	National Institute of Meteorological Research/Korea Meteorological Administration, South Korea	$1.88^{\circ} \times 1.25^{\circ}$
HadGEM2-CC	Met Office Hadley Centre (additional HadGEM2-ES realizations contributed by Instituto Nacional de Pesquisas Espaciais), UK	$1.88^{\circ} \times 1.25^{\circ}$
HadGEM2-ES		
inmcm4	Institute of Numerical Mathematics, Russia	$2^{\circ} \times 1.5^{\circ}$
IPSL-CM5A-LR	Institut Pierre-Simon Laplace, France	$3.75^{\circ} \times 1.89^{\circ}$
IPSL-CM5A-MR		$2.50^{\circ} \times 1.27^{\circ}$
IPSL-CM5B-LR		$3.75^{\circ} \times 1.89^{\circ}$
MIROC5	Atmosphere and Ocean Research Institute (The University of Tokyo), National Institute for Environmental Studies, and Japan Agency for Marine-Earth Science and Technology, Japan	$1.41^{\circ} \times 1.40^{\circ}$
MIROC-ESM	Japan Agency for Marine-Earth Science and Technology, Atmosphere and Ocean Research Institute (The University of Tokyo), and National Institute for Environmental Studies, Japan	$2.81^{\circ} \times 2.79^{\circ}$
MIROC-ESM-CHEM		
MPI-ESM-LR	Max Planck Institute for Meteorology (MPI-M), Germany	$1.88^{\circ} \times 1.86^{\circ}$
MPI-ESM-MR		
MRI-CGCM3	Meteorological Research Institute, Japan	$1.13^{\circ} \times 1.12^{\circ}$
NorESM1-M	Norwegian Climate Centre, Norway	$2.50^{\circ} \times 1.89^{\circ}$

The GCM outputs vary considerably in terms of the spatial resolution and include systematic biases precluding their immediate application to the assessment of climate change impacts. Therefore, certain processes to make up for these limitations are generally required before use. Daily data were downscaled for the period of 1976–2100 and bias-corrected against the observation data from 25 weather stations by using a simple quantile mapping (SQM) method [58]. The SQM technique performs independent refinements by observation points and meteorological variables through empirical quantile mapping. In this study, the following three-step process was used: (1) extract the GCM grid data corresponding to each target station, (2) estimate the biases of the retrospective simulations, and (3) bias-correct the future projections. A single grid covering the target station was extracted for each GCM, and the biases of retrospective simulation outputs for the selected grid were estimated in comparison to observations. The differences between the observed and simulated cumulative distribution functions (CDFs) for the retrospective period were quantified and then applied to the future simulations for a given percentile (Equation (4)):

$$x'_p(t) = x_p(t) + F_{\text{obs}}^{-1}(F_{p,\text{sim}}(x_p(t))) - F_{\text{r.sim}}^{-1}(F_{p,\text{sim}}(x_p(t))) \quad (4)$$

where $x'_p(t)$ and $x_p(t)$ denote the bias-corrected and raw future projections on day t , and $F(\theta)$ and $F^{-1}(\theta)$ are a CDF of the daily data θ and its inverse, respectively. The subscripts *p.sim*, *r.sim*, and *obs* indicate the future projection, retrospective simulation, and observed daily data, respectively.

The non-parametric empirical equation temporally measures the amount of daily observation data and raw GCM data. According to Gudmundsson [59], the nonparametric methods have shown the best skill in reducing the systematic bias compared to the parametric style because these use the real distribution of the observed and simulated data, without estimating a probability distribution function.

2.5. Climate Indices for Evaluations of GCMs

The Joint Expert Team on Climate Change Detection and Indices (ETCCDI) has defined a set of 27 core climate indices mainly focusing on extreme events, which are derived from the daily climate data. In this study, six extreme rainfall-related indices were selected, as shown in Table 4. These indices were used to quantitatively evaluate the future extremes and drought-related rainfall patterns of 29 CMIP5 GCM data. Analyses were conducted for 30-year periods starting from the 2010s, 2040s, and 2070s relative to the 1976–2005 baseline period.

Table 4. List of the ETCCDI extreme climate indices.

ID	Indicator Name	Definition	Unit
PRCPTOT	Annual total wet-day precipitation	Annual total PRCP in wet days ($RR \geq 1$ mm)	mm
CDD	Consecutive dry days	Maximum number of consecutive days with $RR < 1$ mm	days
CWD	Consecutive wet days	Maximum number of consecutive days with $RR \geq 1$ mm	days
R10mm	Number of heavy precipitation days	The annual count of days when $PRCP \geq 10$ mm	days
R1mm	Number of days above 1 mm	The annual count of days when $PRCP \geq 1$ mm	days
SDII	Simple daily intensity index	Annual total precipitation divided by the number of wet days (defined as $PRCP \geq 1.0$ mm) in the year	mm/day

3. Results and Discussion

3.1. Evaluations for Retrospective Simulations of GCMs

In this study, the reproducibility of output from 29 CMIP5 GCMs for the historical period from 1976 to 2005 was evaluated through comparisons with observed data concerning ETCCDI precipitation extreme indices, as shown in Table 4. To validate the performance of the bias correction algorithms, ETCCDI precipitation extreme indices were used. The statistical characteristics of each GCM model have been compared with an observed median to determine the performance of each model before (raw) and after bias-correction, and these results are presented in Figure 4. It was found that the bias-corrected GCM results reasonably captured the observed patterns of ETCCDI precipitation extremes indices, while raw GCM outputs included significant differences from the observed indices. The CDD, CWD, and R1mm of the raw GCM outputs were overestimated by 0.64%, 142.79%, and 11.02%, while R10mm, PRCPTOT, and SDII were underestimated by 43.34%, 59.51%, and 53.19%, respectively. Definitions of the indices are given in Table 4. After bias-correction, most of the errors were removed and only 11.15% and 55.57% of the errors in CDD and CWD remained, which were related to the temporal pattern of a precipitation event.

3.2. GCM Skills in Reproducing Drought Characteristics

Drought event reproducibility from GCM simulations was evaluated through EDI values calculated from the raw and bias-corrected GCM projected rainfall, which was compared with observed EDI values calculated from the BMD data from 1976 to 2005, as shown in Table 5. In this study, the average events from 29 GCMs were considered as historical drought events over 30 years. Results were compared for different BMD stations.

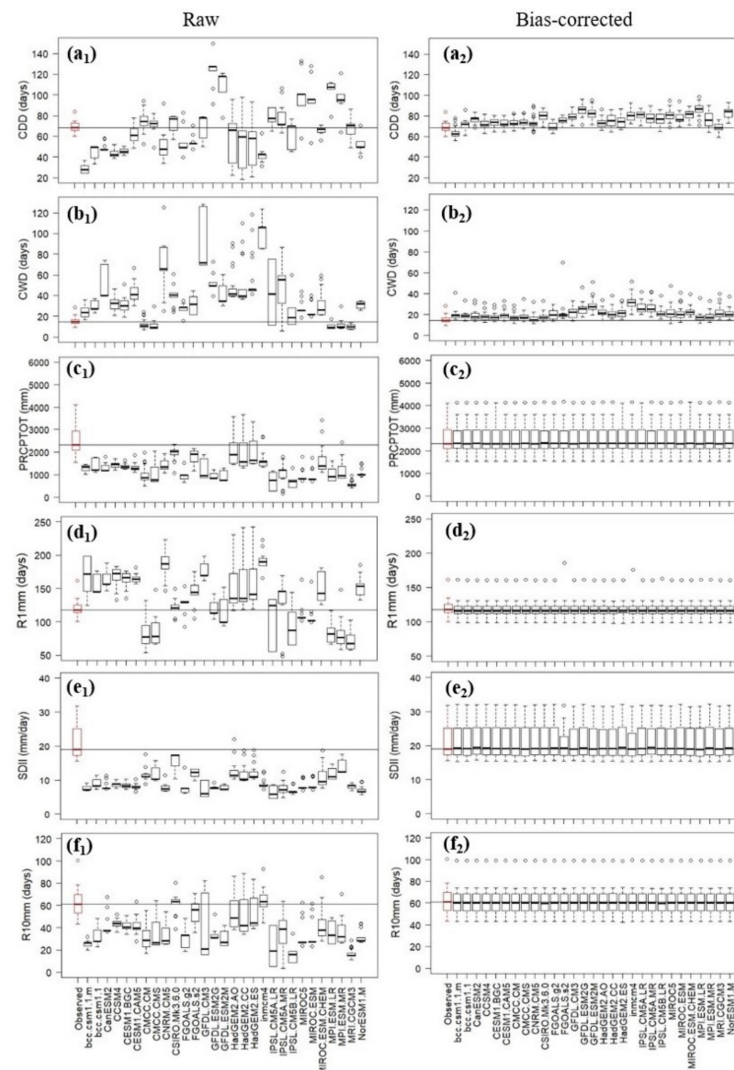


Figure 4. Comparison of raw (left) and bias-corrected (right) reproducibility with observed data for all meteorological stations in terms of the (a) CDD, (b) CWD, (c) PRCPTOT, (d) R1mm, (e) SDII, and (f) R10mm.

Table 5 presents the number of moderate, severe, and extreme drought events that occurred in the past based on observed and modeled results. The results showed that the bias-corrected GCM data could capture the averaged frequencies of moderate and severe droughts over the country quite well, while raw model data underestimated the frequency of moderate droughts by 9% and overestimated that of severe droughts by 5% compared to the observed values. However, bias-correction did not improve the spatial variability of droughts as well as the skills in representing extreme drought events. The number of observed moderate drought events varied within a range of 17–102 over the stations, whereas raw and bias-corrected modeling results showed ranges of 46–55 and 51–58, respectively. Similar limitations in representing the spatial variability of drought events were also found in the case of severe droughts. This was likely due to the issue of the coarse resolution of the GCM itself (Table 3). Specifically, the grid spacing of the GCM configuration may not be detailed enough to present the spatial distributions of the variable (i.e., the frequency) on a station basis.

Table 5. Comparison of several drought events calculated from observed precipitation data and raw and bias-corrected GCM data for 1976–2005. Values in parentheses refer to the standard deviation of the results over the GCMs.

Stations	Moderate Drought			Severe Drought			Extreme Drought		
	Observed	Historical (Raw)	Historical (Bias-Corr.)	Observed	Historical (Raw)	Historical (Bias-Corr.)	Observed	Historical (Raw)	Historical (Bias-Corr.)
Rangpur	43	52 (± 12.3)	58 (± 13.5)	3	8 (± 4.2)	8 (± 2.8)	2	2 (± 1.7)	1 (± 1.2)
Dinajpur	48	50 (± 13.2)	58 (± 13.3)	11	7 (± 4.4)	7 (± 2.7)	4	2 (± 1.8)	1 (± 1.2)
Bogra	54	50 (± 12.0)	51 (± 13.3)	11	8 (± 3.7)	9 (± 2.9)	3	2 (± 1.8)	1 (± 0.8)
Rajshahi	55	46 (± 11.0)	56 (± 11.9)	10	8 (± 4.2)	7 (± 3.5)	3	2 (± 1.6)	1 (± 1.4)
Ishwardi	60	48 (± 08.7)	55 (± 11.2)	5	8 (± 4.0)	8 (± 3.1)	2	2 (± 1.6)	1 (± 1.2)
Jessore	86	47 (± 10.1)	56 (± 10.2)	10	9 (± 4.2)	8 (± 3.4)	2	2 (± 1.6)	2 (± 1.1)
Khulna	65	49 (± 11.4)	52 (± 10.8)	13	9 (± 4.8)	8 (± 3.5)	2	2 (± 1.5)	1 (± 1.0)
Satkhira	65	46 (± 10.6)	54 (± 11.3)	13	9 (± 4.2)	8 (± 3.5)	5	3 (± 1.8)	2 (± 1.4)
Barisal	71	49 (± 11.4)	51 (± 15.1)	20	9 (± 5.0)	9 (± 3.1)	4	2 (± 1.6)	2 (± 1.2)
Patuakhali	21	48 (± 11.8)	57 (± 12.1)	2	9 (± 4.0)	9 (± 3.4)	2	3 (± 1.7)	2 (± 1.4)
Khepupara	60	48 (± 12.4)	54 (± 11.0)	11	9 (± 3.7)	9 (± 3.4)	7	3 (± 1.7)	2 (± 1.3)
Bhola	43	48 (± 12.2)	54 (± 12.8)	8	10 (± 5.1)	9 (± 3.7)	2	2 (± 1.7)	2 (± 1.3)
Maizdicourt	68	52 (± 13.7)	54 (± 13.4)	16	9 (± 5.1)	9 (± 4.1)	1	2 (± 1.4)	2 (± 1.0)
Sawndip	61	54 (± 16.6)	54 (± 17.1)	4	8 (± 4.1)	8 (± 3.3)	3	3 (± 1.8)	2 (± 1.4)
Dhaka	102	47 (± 10.9)	57 (± 10.5)	10	9 (± 4.2)	8 (± 3.2)	3	2 (± 1.9)	2 (± 1.3)
Mymensingh	49	51 (± 14.8)	57 (± 13.4)	12	8 (± 4.4)	8 (± 3.2)	2	2 (± 1.6)	2 (± 1.0)
Hatiya	61	51 (± 15.7)	54 (± 09.7)	2	9 (± 4.6)	8 (± 3.6)	1	2 (± 1.7)	2 (± 1.1)
Chandpur	17	48 (± 11.0)	54 (± 11.5)	0	9 (± 5.0)	7 (± 3.9)	1	2 (± 1.5)	1 (± 0.9)
Comilla	64	52 (± 13.6)	54 (± 13.1)	11	9 (± 4.8)	8 (± 3.3)	4	2 (± 1.5)	1 (± 1.0)
Feni	45	55 (± 14.3)	56 (± 15.5)	6	9 (± 4.9)	9 (± 3.9)	5	2 (± 1.8)	2 (± 1.3)
Sylhet	84	54 (± 14.4)	51 (± 11.8)	9	8 (± 4.6)	9 (± 3.6)	3	2 (± 1.4)	2 (± 1.3)
Srimongal	53	54 (± 13.7)	57 (± 12.8)	5	8 (± 4.1)	8 (± 3.5)	2	2 (± 1.7)	2 (± 1.3)
Rangamati	54	53 (± 15.9)	58 (± 17.3)	9	8 (± 4.1)	7 (± 2.7)	3	2 (± 1.7)	2 (± 1.3)
Cox's bazar	19	46 (± 12.9)	56 (± 13.3)	3	10 (± 3.7)	9 (± 4.2)	1	2 (± 1.5)	2 (± 1.5)
Chittagong	24	52 (± 15.6)	58 (± 15.5)	0	9 (± 4.6)	8 (± 4.0)	0	2 (± 1.9)	2 (± 1.2)
Bangladesh	54.88	49.94	55.04	8.16	8.60	8.2	2.68	2.29	1.68
In percent (%)		Under-estimate 9%	Match		Over-estimate 5%	Match		Under-estimate 15%	Under-estimate 37%

The frequency of observed extreme droughts varied within a range of 0–7 over the stations, while the raw and bias-corrected modeling results showed ranges of 2–3 and 1–2, respectively, during the historical period between 1976 and 2005. As only a few extreme drought events occurred in the past, the model was not able to provide enough indications of such an occurrence. This was likely due to the differences between the observed and GCM temporal patterns of precipitation events such as the CDD and CWD, of which errors remained even after bias-correction (Figure 3). However, bias-corrected GCM data reasonably provided information on severe and moderate droughts. These findings were similarly discussed in the previous study by Hasan et al. [35].

3.3. Changes in Precipitation

This study evaluated how the characteristics of precipitation, which could potentially induce drought events, will change in the future so that we could better illuminate the driving processes underlying changes in droughts. The spatial distributions of averaged precipitation amounts from the MME mean in the 2010s, 2040s, and 2070s were compared to the baseline period (1976–2005) under the RCP4.5 and RCP8.5 scenarios, as shown in Figure 5. The projected percentage change in precipitation was uneven over the entire country, but overall, precipitation tended to increase in the future over Bangladesh.

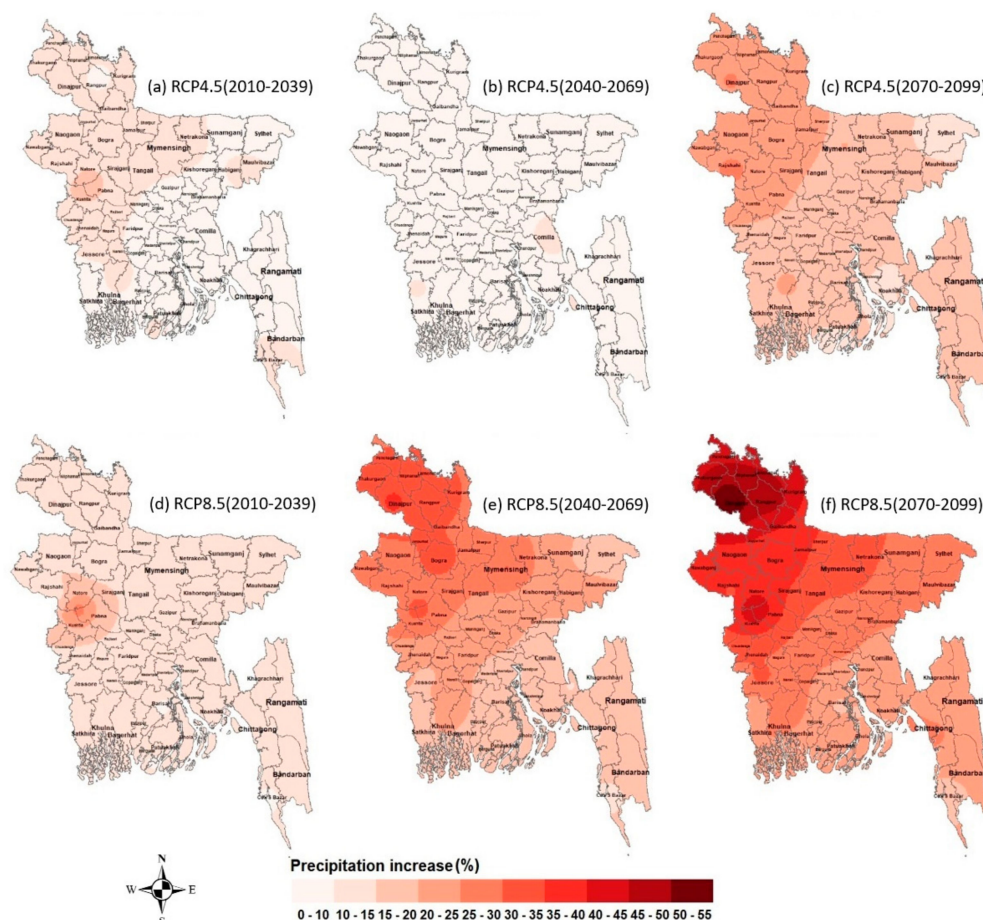


Figure 5. Percentage (%) change of precipitation over Bangladesh for the 2010s (1st column), 2040s (2nd column), and 2070s (3rd column) under the RCP4.5 (upper row) and (2) RCP8.5 (lower row) scenarios relative to the baseline period (1976–2005).

For the beginning of the century (the 2010s), Bangladesh is expected to face an increase of up to 18.72% and 26.23% in precipitation under RCP4.5 and RCP8.5, respectively, compared to the baseline period. In particular, the maximum increases were located on the border between the Natore, Panbna,

and Kustia districts. An increase of up to 14.63% in precipitation was also projected to occur by the middle of the century (the 2040s) under RCP4.5 compared to the baseline period, but the amount was less than that from the 2010s. The highest increases were found in the Shatkhira and Comilla districts, which are located in the southern and eastern regions, respectively. However, the most significant increase of rainfall, up to 35.67%, was projected during the middle of the century (the 2040s) under RCP8.5, especially in the districts in the northern region, and the increasing trend grew more severe with time. Growth of up to 26.14% and 53.95% in precipitation was also projected to occur under RCP4.5 and RCP8.5, respectively, by the end of the century (the 2070s) over Bangladesh. The highest increase in rainfall is expected to happen over the northern region of Bangladesh, especially the Dinajpur and Rajshahi districts.

Overall, the dominant feature detected was that the widespread precipitation will be increased in the 21st century over Bangladesh, especially under the RCP8.5 scenario. This result agreed with the previous study by Fahad et al. [60]. The increasing trend of precipitation may generally imply a decrease in drought occurrence.

The future changes in climate indices (PRCPTOT, CWD, CDD, R10mm, R1mm, and SDII) calculated by using data from the 29 GCMs for RCP4.5 and RCP8.5 were further investigated, as shown in Figure 6. When comparing the median values of the box and whisker diagrams, most of the climate indices showed changes indicative of increasing severity of precipitation (i.e., more precipitation with a lower number of rainy days). According to Figure 6c, the total annual precipitation (PRCPTOT) tended to increase gradually in the three future periods under both RCP scenarios; PRCPTOT increased at the end of the century (the 2070s) by around 31.98% under the RCP8.5 scenario compared to the baseline period followed by about 17.66% under the RCP4.5 scenario in the same period. Conversely, the number of rainy days (R1mm) decreased in the middle (the 2040s) and end of the century (the 2070s) by around 0.51% and 0.61%, respectively, under RCP8.5 and by 0.49% at the beginning of the century under RCP4.5 compared to the baseline period, as shown in Figure 6d. This finding was related to the gradual increase of the simple daily rainfall intensity (SDII) and heavy rainfall events ($\text{PRCP} \geq 10 \text{ mm}$), as shown in Figure 6e,f.

Changes in the frequency of precipitation events were also manifest as changes in the duration of dry spells (consecutive dry days, CDD) and wet spells (consecutive wet days, CWD). The CDD will be increased in the three future periods under both scenarios, as shown in Figure 6a. The highest CDD rise occurred at the end of the century (the 2070s) by around 12.08% under the RCP8.5 scenario compared to the baseline period followed by approximately 9.57% in the middle of the century (2040s) under the same scenario. However, the lowest CDD increase occurred at the beginning of the century (the 2010s) by around 4.83% under the RCP8.5 scenario compared to the base period. The CWD is also expected to show a minimum increase in the 21st century with a range of 1.12 to 2.37% compared to the base period as shown in Figure 6b. The highest CWD increase occurred at the end of the century (2070) under the RCP8.5 scenario, while the lowest rise occurred in the middle of the century (the 2040s) under the RCP4.5 scenario. Previously, Hasan et al. [37] also projected that heavy rainfall is expected to increase in the future.

Generally, the change in extreme precipitation index patterns confirms the increasing trend of precipitation in the future. Moreover, a decrease in the number of drought events and a reduction of long-term drought duration can be expected given the related increases in total precipitation in Bangladesh. However, the CDD will be increased, which may lead to an increase in extreme drought events as well as extreme drought days in the future. However, the model used in this study cannot provide the real essence of changes in extreme drought events (Table 5).

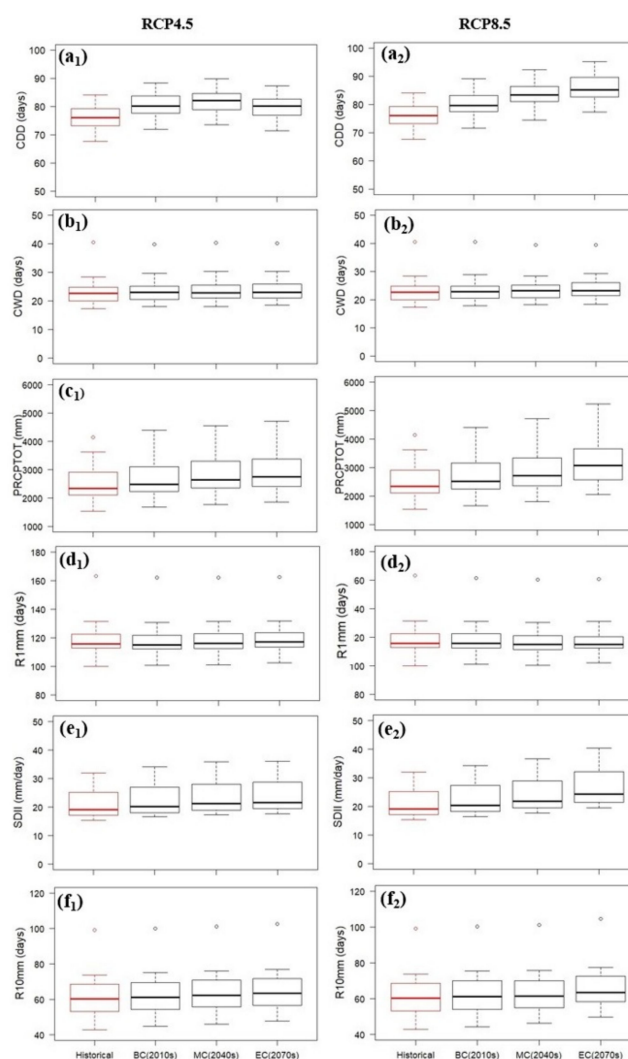


Figure 6. Future changes of climate indices under RCP4.5 (left) and RCP8.5 (right); (a) CDD, (b) CWD, (c) PRCPTOT, (d) R1mm, (e) SDII, and (f) R10mm.

3.4. Projections of Future Changes in Drought Characteristics

Future climatological changes in drought frequency, mean duration, and maximum intensity was investigated by using the GCM simulations in the 2010s, 2040s, and 2070s compared to the baseline period (1976–2005) under the RCP4.5 and RCP8.5 scenarios. To compute the differences between baseline and future drought characteristics, the percent change for the three next periods under each scenario were calculated by counting the number of events for each level of drought severity and duration for the three future periods under both scenarios.

3.4.1. Changes in the Drought Frequency

Figure 7 compares the drought frequency for each level of drought severity (i.e., extreme, severe, and moderate drought events) and future periods under the RCP4.5 and RCP8.5 scenarios. Overall, the projected changes in drought frequency for the three future periods showed different characteristics. However, the respective change in climatological severity under RCP4.5 and RCP8.5 exhibited a constant magnitude response for any future period, thus indicating an insignificant effect of emission scenarios on the projected change in extreme and severe droughts. Besides, extreme droughts are not expected to change much in the 21st century under both scenarios.

According to Figure 7, it was found that the MME mean produced the maximum number of moderate drought events compared to the others. For the beginning of the century (the 2010s), moderate

droughts decreased by around 9% and 14% under RCP4.5 and RCP8.5, respectively. However, only severe droughts increased by about 15% under both of the scenarios. Moreover, moderate droughts decreased by about 18% in the middle of the century (the 2040s) compared to the base period under both of the scenarios, while severe droughts are expected to remain the same under both scenarios. Furthermore, the moderate and severe droughts events are expected to decrease by around 29% and 12%, respectively, at the end of the century (the 2070s) compared to the base period under the RCP4.5 scenario, while 38% of moderate and 23% of severe drought events will decrease in the same period under the RCP8.5 scenario.

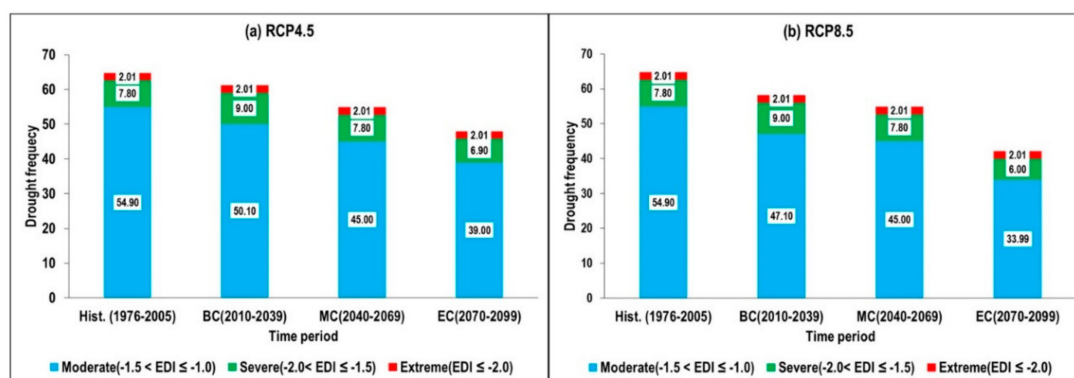


Figure 7. Change in the drought intensity based on a historical period (1976–2005) in regard to extreme, severe, and moderate drought events under the (a) RCP4.5 (left) and (b) RCP8.5 (right) scenarios.

The spatial distributions of climatological changes in drought frequency for the future periods are shown in Figure 8. The projected percentage change in drought frequency was non-uniform over the country. However, the overall drought frequency will likely decrease with time under climate change. The CMIP5 does not well capture the spatial variability in Bangladesh, as discussed in Table 5. Therefore, the spatial distributions analyzed here may contain large uncertainty.

For the beginning of the century (the 2010s), the drought frequency appeared to decrease in most of the country. In particular, the maximum decrease was detected in the eastern mountainous regions, especially the Chittagong and Bandarban districts, with ranges up to 10–15% compared to the base period under the RCP4.5 scenario. However, it increased up to 3% in the districts of Jessore and Satkhira, but only under RCP4.5, by the 2010s compared to the base period. On the other hand, the drought frequency decreased all over the country under the RCP8.5 scenario. The highest decrease was detected in the districts of Noakhali, Hobigonj, and Moulvibazar during the 2010s. Furthermore, a decrease of up to 23% in drought frequency was also projected to occur by the middle of the century (the 2040s) under RCP4.5 compared to the baseline period, which was greater than that from the 2010s. The highest decrease was detected in the districts of Mymensingh and Chittagong. A decrease in frequency, up to 24%, was projected to occur over Bangladesh during the middle of the century (the 2040s) under RCP8.5, especially in the eastern region. A greater decrease in frequency can be expected over Bangladesh for the 2070s than for the 2010s and 2040s. A decrease of up to 33.33% and 46.77% in drought frequency was also projected under RCP4.5 and RCP8.5, respectively, to occur by the end of the century (the 2070s) over Bangladesh relative to the baseline period of 1976–2005. The highest decrease in frequency was projected to occur over the drought-vulnerable northern and northeastern regions of Bangladesh, especially in the Rajshahi and Sylhet districts.

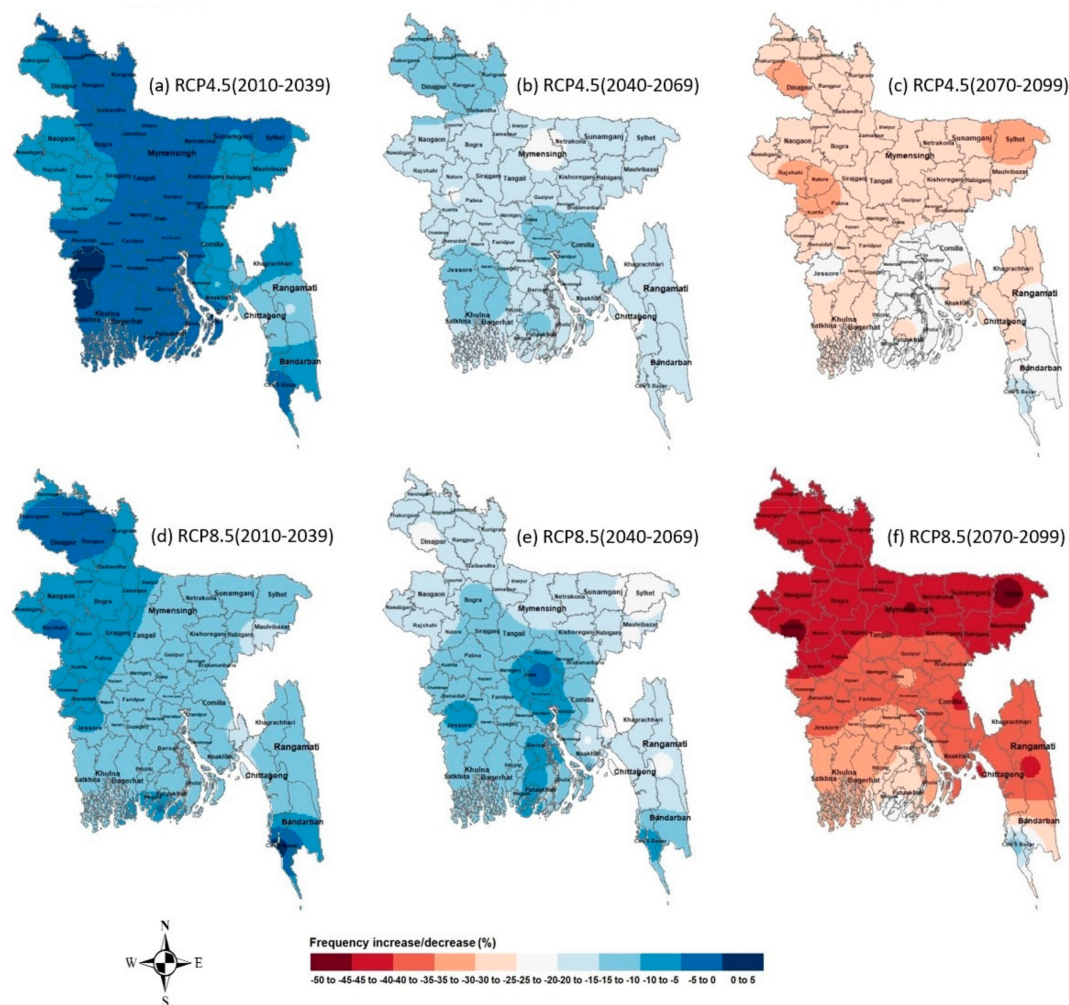


Figure 8. Percentage (%) change in the drought frequency over Bangladesh for the 2010s (1st column), 2040s (2nd column), and 2070s (3rd column) under the RCP4.5 (upper row) and RCP8.5 (lower row) scenarios relative to the baseline period (1976–2005).

3.4.2. Changes in the Drought Duration

Figure 9 presents the changes in drought duration for the 21st century based on the historical period (1976–2005) concerning long-term, medium-term, short-term, and very short-term drought events under the RCP4.5 and RCP8.5 scenarios. Overall, the projected changes in drought duration for the three future periods (the 2010s, 2040s, and 2070s) showed different characteristics. However, the respective change in the climatological length of droughts under RCP4.5 and RCP8.5 exhibited a stable magnitude for any future period, thus showing a negligible effect of emission scenarios. The medium-term droughts are not expected to change in the 21st century under both scenarios except by the end of the century (the 2070s) under RCP8.5, where a decrease of 55% was detected compared to the base period. Only the long-term droughts will decrease by around 55% over the three future periods under both scenarios compared to the base period.

According to Figure 9, The short-term and very short-term droughts will be decreased in the 21st century under both scenarios except for at the beginning of the century (the 2010s) under RCP4.5. The highest decreasing rates of very short-term and short-term drought events can be expected at the end of the century and will amount to around 26% and 21%, respectively, compared to the base period under the RCP4.5 scenario, while 36% of the very short-term and 31% of the short-term drought events decreased in the same period under the RCP8.5 scenario.

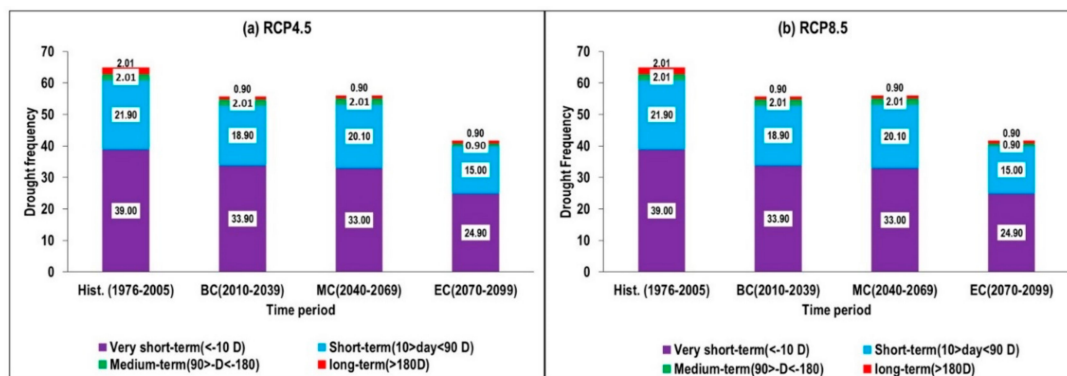


Figure 9. Change in the drought duration based on a historical period (1976–2005) in regard to long-term, medium-term, short-term, and very short-term drought events under the (a) RCP4.5 (left) and (b) RCP8.5 (right) scenarios.

The mean duration of droughts was computed from the average duration of all drought events in the historical and three future periods with the MME mean of the GCMs. The climatological changes in mean drought duration for the future periods are shown in Figure 10. The difference is a percentage that designates the change in the mean duration of droughts, where a negative value indicates a decreasing trend and vice versa. The average length of droughts can be expected to decline in the 21st century all over the country. However, the decreasing rate varied with the projected period, location, and emission scenario. The results indicate that the decreasing rate will be increased with time and the highest decreasing rate can be expected during the end of the century (the 2070s) under RCP4.5.

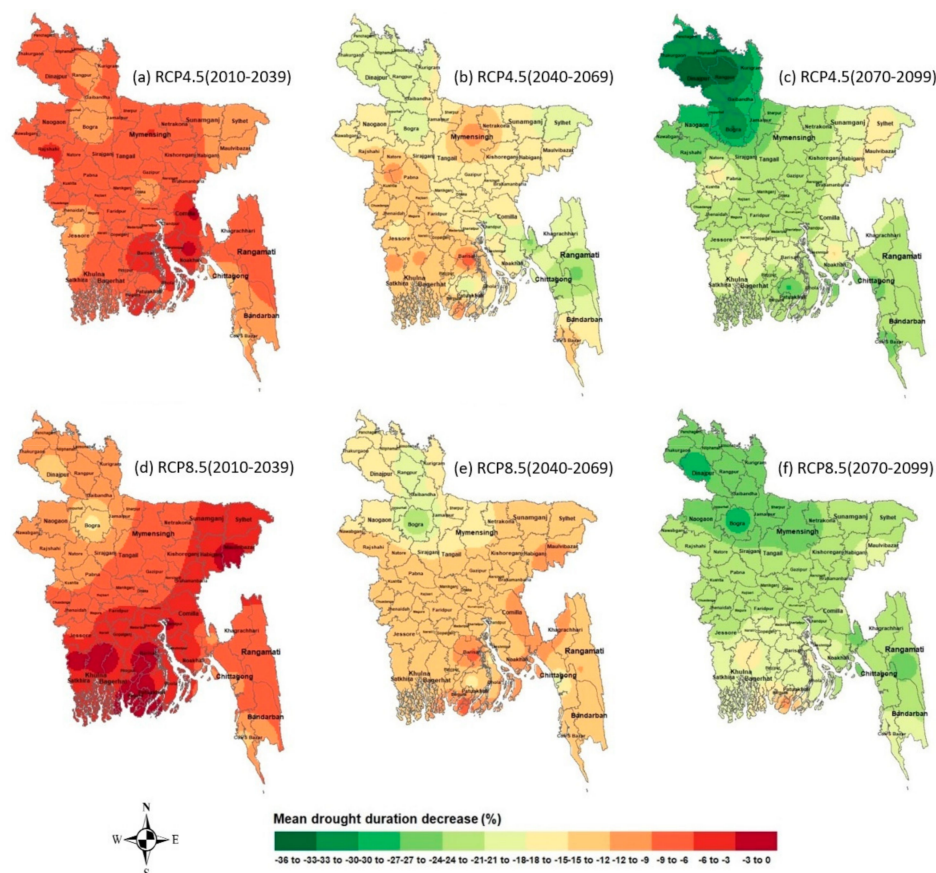


Figure 10. Percentage (%) change in the mean drought duration over Bangladesh for the 2010s (1st column), 2040s (2nd column), and 2070s (3rd column) under the RCP4.5 (upper row) and RCP8.5 (lower row) scenarios relative to the baseline period (1976–2005).

In particular, the mean duration of droughts is expected to decrease within a range of 0 to 15% over the entire country, whereas the highest decrease will occur in the districts of Chittagong, Cox's Bazar, and Jessore at the beginning of the century (the 2010s). The values decreased within a range of 6–24% and 14–36% in the middle of the century (the 2040s) and end of the century (2070s), respectively, under the RCP4.5 scenario. The highest decreases occurred in the hilly district of Rangamati in the 2040s and in the Rangpur and Dinajpur districts in the 2070s. On the other hand, the RCP8.5 scenario results tended to show a higher decreasing rate in the northern region, especially in the Bogra district. In particular, the mean duration of droughts decreased within a range of 0 to –16% all over the country at the beginning of the century (the 2010s), and decreases occurred within a range of 6–24% and 10–28% in the middle of the century (the 2040s) and end of the century (2070s), respectively, under the RCP8.5 scenario.

3.4.3. Changes in the Drought Intensity

The intensity of the EDI was computed from the MME means derived from the GCMs, and resulting data were used to assess the extreme intensity trends (minimum values of the EDI) among all of the drought events in the three future periods compared to the historical period (1976–2005). The difference is a percentage designating the change in maximum intensity of droughts, where a positive value indicates an increasing trend and vice versa. The climatological changes in the maximum drought intensity for future periods are shown in Figure 11. Overall, the projected change in maximum drought intensity for the three future periods showed different characteristics. The maximum drought intensity increased over most of the country at the beginning of the century (the 2010s). However, a greater decrease can be expected for the end of the century (the 2070s) under RCP8.5.

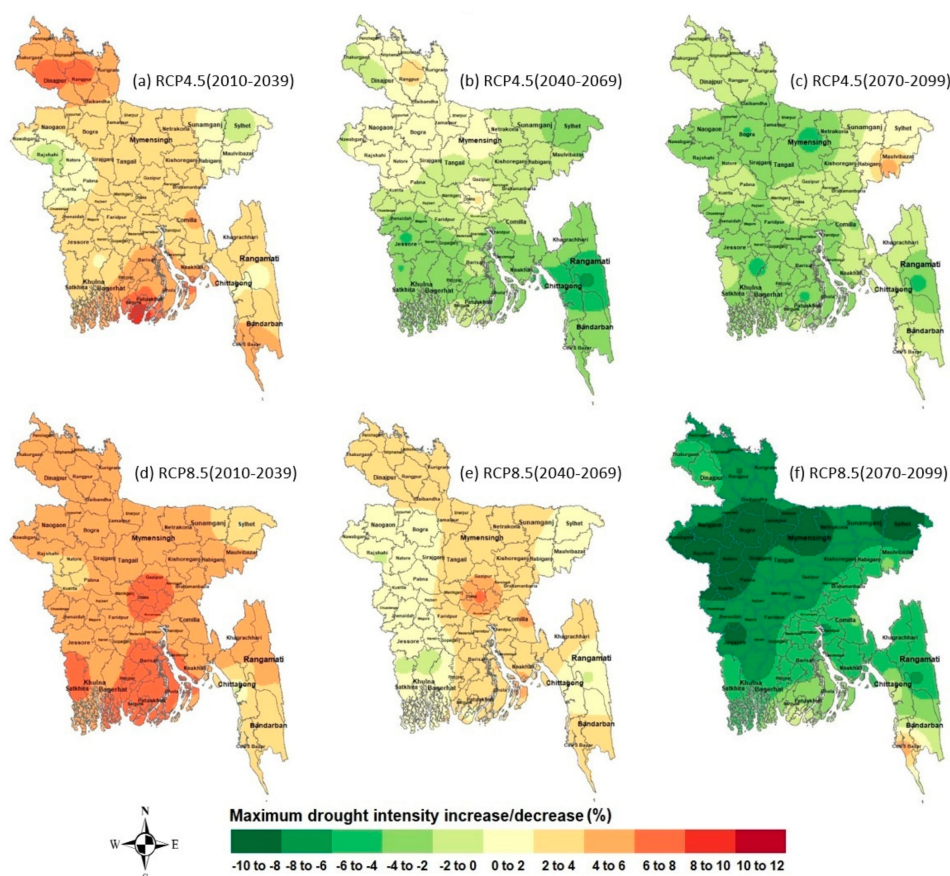


Figure 11. Percentage (%) change in the maximum drought intensity over Bangladesh for the 2010s (1st column), 2040s (2nd column), and 2070s (3rd column) under the RCP4.5 (upper row) and RCP8.5 (lower row) scenarios relative to the baseline period (1976–2005).

In particular, the maximum increase occurred in northern and southwestern coastal regions, especially the Borguna district, with ranges up to 8–10% under the RCP4.5 scenario, whereas a maximum increase up to 6–8% was also projected under the RCP8.5 scenario, in locations including the southwestern and central regions, during the beginning of the century compared to the base period. However, values decreased up to 1–2% in the districts of Rajshahi and Sylhet only under RCP4.5 in the 2010s, and negligible decreases were detected under the RCP8.5 scenario.

Besides, the maximum drought intensity for the middle of the century showed a tendency to decrease under RCP4.5 but an increasing trend under RCP8.5. Precisely, a decrease of up to 6–8% in the drought intensity is projected to occur by the middle of the century (the 2040s) under RCP4.5 compared to the baseline period. The higher decrease was located in the hilly eastern region and southwestern coastal region, especially in the districts of Rangamati and Chittagong. Conversely, an increase in the intensity of up to 6–8% was projected to occur over Bangladesh during the middle of the century (the 2040s) under RCP8.5, especially in the central region.

A decrease of up to 4–6% and 8–10% in the maximum drought intensity was also projected under RCP4.5 and RCP8.5, respectively, by the end of the century (the 2070s) over Bangladesh relative to the baseline period of 1976–2005. The highest decrease in intensity was detected over the drought-vulnerable northern region and northeastern region of Bangladesh, especially in the Rajshahi and Sylhet districts under the RCP8.5 scenario.

3.5. Projections of Seasonal Changes in the Number of Drought Days

In this study, the changes in moderate, severe, and extreme drought days were investigated during the Pre-Kharif, Kharif, and Rabi seasons for the 2010s, 2040s, and 2070s compared to the baseline period (1976–2005) under the RCP4.5 and RCP8.5 scenarios. The different categories of drought days were counted by using EDI values based on the MME means of 29 GCMs under both scenarios. The drought days estimated at different stations are presented by using box plots. The 25th and 75th quartiles of drought days are demarked by the lower and upper lines of the boxes, whereas the median value drought days are indicated by the middle lines of the boxes at different stations over Bangladesh. The changes in drought days for the Pre-Kharif, Kharif, and Rabi drought seasons are shown in Figure 12. Overall, an increase of median values of extreme drought days was observed with some exceptions, whereas the opposite trends in moderate and severe drought days were detected under both scenarios compared to the base period.

Particularly, the maximum decrease in the moderate and severe drought days was found in the Rabi season with changes of around 50% and 44% under RCP4.5 and 44% and 53% under RCP8.5, respectively, during the end of the century (the 2070s) compared to the base period. However, the severe droughts days increased at the beginning of the century in the Pre-Kharif and Kharif seasons by around 28% and 3%, respectively, under RCP4.5, and 12% in the Pre-Kharif season under RCP8.5. The moderate drought days are expected to increase at the beginning of the century in the Pre-Kharif and Kharif seasons by 14% and 7% under RCP4.5, respectively, and 6% in the middle of the century under RCP8.5, respectively. However, values are not expected to increase in the future under the RCP4.5 scenario. Only 30% of the extreme drought days will be decreased in the Kharif season in the middle of the century under RCP4.5, while 17% and 10% decreases are expected in the Kharif and Rabi seasons, respectively, at the end of the century under the RCP8.5 scenario. The highest increase in extreme drought days was found in the Pre-Kharif season, and the increase was around 205% at the end of the century under RCP4.5.

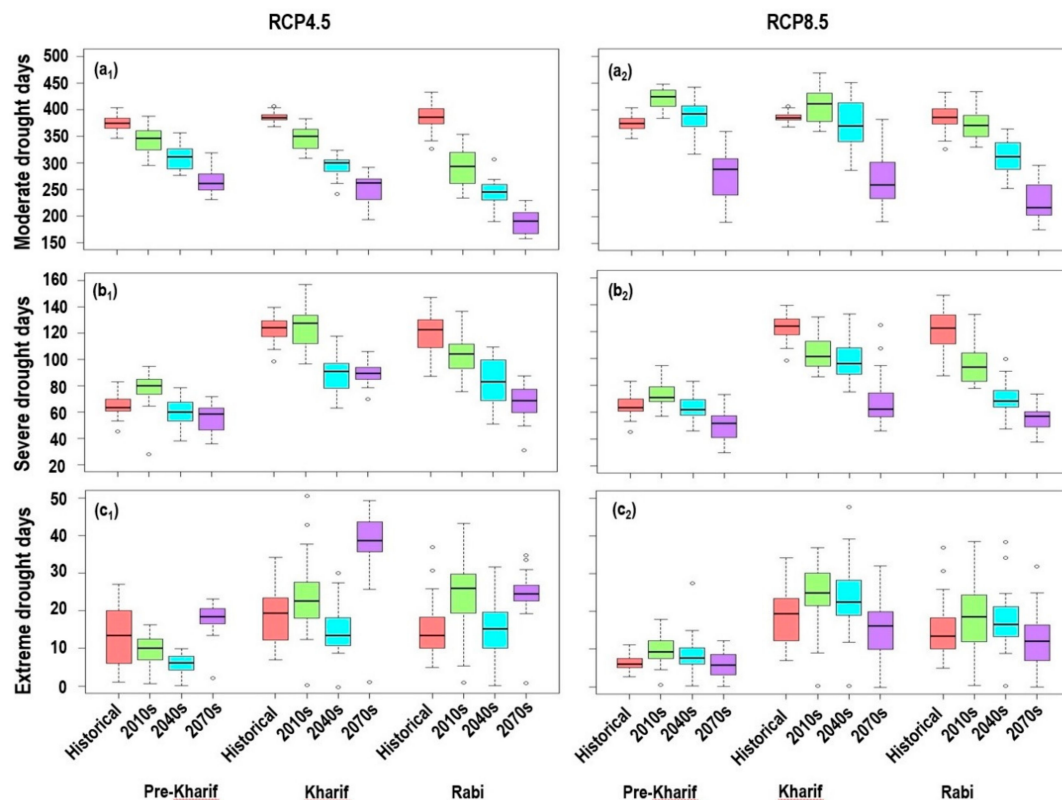


Figure 12. Future changes in seasonal drought days under RCP4.5 (left) and RCP8.5 (right); (a) moderate, (b) severe, and (c) extreme droughts.

4. Conclusions

Climate change is regarded as a future threat that is expected to change regional hydrological patterns as well as the characteristics of droughts, which could lead to severe drought-related disasters. Hence, it is important to assess the impacts of climate change on potential future droughts. Such work will allow us to respond preventively by providing policy analysis information and useful guidance to policymakers, who can devise a framework for water resource management as well as agricultural adaptation in the future. In this regard, the principal objectives of this study were to evaluate the changes in drought-related precipitation extremes and drought characteristics over Bangladesh by using 29 GCM projections under the RCP4.5 and RCP8.5 scenarios for the period of 2010–2099. The Effective Drought Index (EDI) was used for the characterization of droughts in terms of the frequency, duration, intensity, and number of drought days. To evaluate the reproducibility of the GCMs, retrospective simulations of models for the historical period from 1976 to 2005 were compared to the quantities based on observed climatology. It was found that the bias-corrected GCM results showed an appropriate consistency with observation data and were successfully able to reproduce the real essence of the drought situation compared to the raw GCM data except for extreme drought events. Future changes of drought characteristics were then investigated for the entire area by using the historical period as the calibration period. The differences between climate change scenarios were not recognizable from the results because a statistical trend analysis was not included in the study. The changes in drought characteristics in the future were examined only through comparisons with the historical period. The increasing or decreasing trends of future precipitation and drought characteristics were visually inspected in this study.

The future changes in precipitation tended to show increases under both scenarios; the increasing rate was higher under RCP8.5 than RCP4.5. The projected change in climatological frequencies of drought based on severity and duration under RCP4.5 and RCP8.5 exhibited a consistent magnitude for any future period, thus indicating a negligible effect of emission scenarios on the projected changes

in the extreme and severe droughts and long-term and medium-term droughts. Overall, the drought frequency, mean duration, and maximum intensity will likely decrease with time under climate change in relation to the increase of total precipitation. In particular, the occurrence of severe and moderate droughts will be less frequent in the 21st century, according to this research. The frequency of extreme drought events did not show a significant change in the 21st century under both scenarios. However, the extreme drought days are likely to be increased in most of the cropping season and future periods under both scenarios, which may affect agricultural production in the future, as driven by the increasing pattern of CDD. The spatial pattern of change in drought characteristics indicates that the drought-vulnerable areas will be shifted from the northwestern to central and southern coastal regions in the future due to the effects of climate change. However, GCM may predict the trends well but may not reveal the change in a spatial pattern in detail.

Lastly, to our best of knowledge, this study is the first attempt to characterize the future droughts in Bangladesh widely using the EDI. The present results can help resource managers to optimally allocate scarce water resources and develop long-term strategies for protecting communities against natural hazards related to water scarcity. Furthermore, the outcomes of the study are expected to represent important measures for mitigating the losses in agricultural production for drought-prone areas in Bangladesh.

Author Contributions: M.K. and M.-W.J. are equal contributions as a first author; M.K. and S.H. designed the research, analyzed the data, and wrote the manuscript; M.-W.J. helped in the preparation of the manuscript and subsequent revisions; J.C. provided important intellectual content; S.H. supervised the study and providing critical evaluations of the manuscript.

Funding: This research was funded by Research Program for Agricultural Science & Technology Development, National Institute of Agricultural Sciences, Rural Development Administration, Korea, project number PJ01254903.

Acknowledgments: The authors are grateful to the Bangladesh Meteorological Department (BMD) for providing the rainfall data.

Conflicts of Interest: The authors declare no conflict of interest.

References

- Basak, J.K.; Titumir, R.A.M.; Dey, N.C. Climate Change in Bangladesh: A Historical Analysis of Temperature and Rainfall Data. *J. Environ.* **2013**, *2*, 41–46.
- Ahmad, Q.K.; Warrick, R.A.; Ericksen, N.J.; Mirza, M.Q. *The Implications of Climate and Sea-Level Change for Bangladesh*; Warrick, R.A., Ahmad, Q.K., Eds.; Kluwer Academic Publisher: Dordrecht, The Netherlands, 1996; ISBN 978-94-009-0241-1.
- Shahid, S. Recent trends in the climate of Bangladesh. *Clim. Res.* **2010**, *42*, 185–193. [[CrossRef](#)]
- Rahman, M.R.; Lateh, H. Climate change in Bangladesh: A spatiotemporal analysis and simulation of recent temperature and rainfall data using GIS and time series analysis model. *Appl. Clim.* **2017**, *128*, 27–41. [[CrossRef](#)]
- Dai, A. Drought under global warming: A review. *Wiley Interdiscip. Rev. Clim. Chang.* **2011**, *2*, 45–65. [[CrossRef](#)]
- Brown, C.; Meeks, R.; Hunu, K.; Yu, W. Hydro climatic risk to economic growth in sub-Saharan Africa. *Clim. Chang.* **2011**, *106*, 621–647. [[CrossRef](#)]
- Hartmann, D.L.; Tank, A.M.G.K.; Rusticucci, M. *Climatic Change 2013: The Physical Science Basis*; IPCC Fifth Assessment Report; IPCC: Geneva, Switzerland, 2013; pp. 31–39.
- Inter-Governmental Panel on Climate Change (IPCC). Summary for Policymakers. In *Climate Change 2013: The Physical Science Basis*; Contribution of Working Group I to the Fifth Assessment Report of IPCC; Cambridge University Press: Cambridge, UK; New York, NY, USA, 2013.
- Solomon, S. (Ed.) *Climate Change—The Physical Science Basis: Working Group I Contribution to the Fourth Assessment Report of the IPCC 4*; Cambridge University Press: Cambridge, UK; New York, NY, USA, 2007.
- Van Vuuren, D.P.; Edmonds, J.; Kainuma, M. The representative concentration pathways: An overview. *Clim. Chang.* **2011**, *109*, 5–31. [[CrossRef](#)]

11. Taylor, K.E.; Stouffer, R.J.; Meehl, G.A. An overview of CMIP5 and the experiment design. *Bull. Am. Meteorol. Soc.* **2012**, *93*, 485–498. [\[CrossRef\]](#)
12. Sperber, K.R.; Annamalai, H.; Kang, I.S.; Kitoh, A.; Moise, A.; Turner, A.; Zhou, T. The Asian summer monsoon: An intercomparison of CMIP5 vs. CMIP3 simulations of the late 20th century. *Clim. Dyn.* **2013**, *41*, 2711–2744. [\[CrossRef\]](#)
13. Bhaskaran, B.; Ramachandran, A.; Jones, R.; Moufouma-Okia, W. Regional climate model applications on sub-regional scales over the Indian monsoon region: The role of domain size on downscaling uncertainty. *J. Geophys. Res. Atmos.* **2012**, *117*. [\[CrossRef\]](#)
14. Xu, C.Y.; Widen, E.; Halldin, S. Modelling hydrological consequences of climate change-progress and challenges. *Adv. Atmos. Sci.* **2005**, *22*, 789–797. [\[CrossRef\]](#)
15. Fowler, H.J.; Kilsby, C.G. Using regional climate model data to simulate historical and future river flows in northwest England. *Clim. Chang.* **2007**, *80*, 337–367. [\[CrossRef\]](#)
16. Hong, S.Y.; Kanamitsu, M. Dynamical downscaling: Fundamental issues from an NWP point of view and recommendations. *Asia Pac. J. Atmos. Sci.* **2014**, *50*, 83–104. [\[CrossRef\]](#)
17. Kang, S.; Hur, J.; Ahn, J.B. Statistical downscaling methods based on APCC multi-model ensemble for seasonal prediction over South Korea. *Int. J. Clim.* **2014**, *34*, 3801–3810. [\[CrossRef\]](#)
18. Lee, J.W.; Hong, S.Y. Potential for added value to downscaled climate extremes over Korea by increased resolution of a regional climate model. *Theor. Appl. Climatol.* **2014**, *117*, 667–677. [\[CrossRef\]](#)
19. Kunkel, K.E.; Liang, X.Z.; Zhu, J.; Lin, Y. Can CGCMs simulate the twentieth-century “warming hole” in the central United States? *J. Clim.* **2006**, *19*, 4137–4153. [\[CrossRef\]](#)
20. Fowler, H.J.; Blenkinsop, S.; Tebaldi, C. Linking climate change modeling to impacts studies: Recent advances in downscaling techniques for hydrological modeling. *Int. J. Clim.* **2007**, *27*, 1547–1578. [\[CrossRef\]](#)
21. Hay, L.E.; Wilby, R.L.; Leavesley, G.H. A comparison of delta change and downscaled GCM scenarios for three mountainous basins in the United States. *J. Am. Water Resour. Assoc.* **2000**, *36*, 387–397. [\[CrossRef\]](#)
22. Wood, A.W.; Maurer, E.P.; Kumar, A.; Lettenmaier, D.P. Long-range experimental hydrologic forecasting for the eastern United States. *J. Geophys. Res.* **2002**, *107*, 4429. [\[CrossRef\]](#)
23. Heo, J.H.; Ahn, H.; Shin, J.Y.; Kjeldsen, T.R.; Jeong, C. Probability Distributions for a Quantile Mapping Technique for a Bias Correction of Precipitation Data: A Case Study to Precipitation Data Under Climate Change. *Water* **2019**, *11*, 1475. [\[CrossRef\]](#)
24. Zhao, T.; Dai, A. Uncertainties in historical changes and future projections of drought. Part II: Model-simulated historical and future drought changes. *Clim. Chang.* **2016**, *144*, 535–548. [\[CrossRef\]](#)
25. Cohelo, C.A.S.; Goddard, L. El Niño-Induced Tropical Droughts in Climate Change Projections. *J. Clim.* **2009**, *22*, 6456–6476. [\[CrossRef\]](#)
26. Rhee, J.; Cho, J. Future Changes in Drought Characteristics: Regional Analysis for South Korea under CMIP5 Projections. *J. Hydrometeorol.* **2016**, *17*, 437–451. [\[CrossRef\]](#)
27. Touma, D.; Ashfaq, M.; Nayak, M.A.; Kao, S.C.; Dittenbach, N.S. A multi-model and multi-index evaluation of drought characteristics in the 21st century. *J. Hydrol.* **2015**, *526*, 196–207. [\[CrossRef\]](#)
28. Dai, A. Increasing drought under global warming in observations and models. *Nat. Clim. Chang.* **2013**, *3*, 52–58. [\[CrossRef\]](#)
29. Orłowsky, B.; Seneviratne, S.I. Elusive drought: Uncertainty in observed trends and short- and long-term CMIP5 projections. *Hydrol. Earth Syst. Sci.* **2013**, *17*, 1765–1781. [\[CrossRef\]](#)
30. Chen, H.P.; Sun, J.Q.; Chen, X.L. Future changes of drought and flood events in China under a global warming scenario. *Atmos. Ocean. Sci. Lett.* **2013**, *6*, 8–13. [\[CrossRef\]](#)
31. Wang, L.; Chen, W.; Zhou, W. Assessment of future drought in Southwest China based on CMIP5 multimodal projections. *Adv. Atmos. Sci.* **2014**, *31*, 1035–1050. [\[CrossRef\]](#)
32. Burke, E.J.; Brown, S.J. Evaluating uncertainties in the projection of future drought. *J. Hydrometeorol.* **2008**, *9*, 292–299. [\[CrossRef\]](#)
33. Nowreen, S.; Murshed, S.B.; Islam, A.K.M.S. Changes of rainfall extremes around the haor basin areas of Bangladesh using multi-member ensemble RCM. *Appl. Clim.* **2015**, *119*, 363–377. [\[CrossRef\]](#)
34. Rahman, M.M.; Islam, M.N.; Ahmed, A.U.; Georgi, F. Rainfall and temperature scenarios for Bangladesh for the middle of 21st century using RegCM. *J. Earth. Syst. Sci.* **2012**, *121*, 287–295. [\[CrossRef\]](#)

35. Hasan, M.A.; Saiful Islam, A.K.M.; Bokhtiar, S.M. Future change of the metrological drought over Bangladesh using high-resolution climate scenarios. In Proceedings of the International Conference on Climate Change Impact and Adaptation (I3CIA-2013), Gazipur, Bangladesh, 15–17 November 2013.
36. Islam, A.R.M.T.; Shen, S.; Hu, Z.; Rahman, M.A. Drought Hazard Evaluation in Boro Paddy Cultivated Areas of Western Bangladesh at Current and Future Climate Change Conditions. *Adv. Meteorol.* **2017**, *2017*, 3514381. [[CrossRef](#)]
37. Hasan, M.A.; Saiful Islam, A.K.M.; Akanda, A.S. Climate projections, and extremes in dynamically downscaled CMIP5 model output over the Bengal delta: A quartile based bias-correction approach with new gridded data. *Clim. Dyn.* **2018**, *51*, 2169–2190. [[CrossRef](#)]
38. Mortuza, M.R.; Moges, E.; Demissie, Y.; Hong-Yi, L. Historical and future drought in Bangladesh using copula-based bivariate regional frequency analysis. *Appl. Clim.* **2019**, *135*, 855–871. [[CrossRef](#)]
39. McKee, T.B.; Doesken, N.J.; Kleist, J. The relationship of drought frequency and duration to time scales. Preprints. In Proceedings of the Eighth Conference on Applied Climatology, Anaheim, CA, USA, 17–22 January 1993; pp. 179–184.
40. Byun, H.R.; Kim, D.W. Comparing the Effective Drought Index and the Standardized Precipitation Index. In: López-Francos, A. (comp.), López-Francos, A. (collab.). Zaragoza: CIHEAM/FAO/ICARDA/GDAR/CEIGRAM/MARM. *Econ. Drought Drought Prep. A Clim. Chang. Context* **2010**, *95*, 85–89.
41. Byun, H.R.; Wilhite, D.A. Objective quantification of drought severity and duration. *J. Clim.* **1999**, *12*, 2747–2756. [[CrossRef](#)]
42. Morid, S.; Smakhtin, V.; Moghaddasi, M. Comparison of Seven Meteorological drought indices for drought monitoring in Iran. *Int. J. Climatol.* **2006**, *26*, 971–985. [[CrossRef](#)]
43. Pandey, R.P.; Dash, B.B.; Mishra, S.K.; Singh, R. Study of indices for drought characterization in KBK districts in Orissa (India). *Hydrol. Process.* **2008**, *22*, 1895–1907. [[CrossRef](#)]
44. Dogan, S.; Berkday, A.; Singh, V.P. Comparison of multi-monthly rainfall-based drought severity indices, with application to semi-arid Kenya, closed basin, Turkey. *J. Hydrol.* **2012**, *470*, 255–268. [[CrossRef](#)]
45. Jain, V.K.; Pandey, R.P.; Jain, M.K.; Byun, H.R. Comparison of drought indices for appraisal of drought characteristics in the Ken River Basin. *Weather Clim. Extrem.* **2015**, *8*, 1–11. [[CrossRef](#)]
46. Kamruzzaman, M.; Cho, J.; Jang, M.; Hwang, S. Comparative Evaluation of Standardized Precipitation Index (SPI) and Effective Drought Index (EDI) for Meteorological Drought Detection over Bangladesh. *J. Korean Soc. Agric. Eng.* **2019**, *61*, 143–157. [[CrossRef](#)]
47. Mondal, M.A.H.; Ara, I.; Das, S.C. Meteorological Drought Index Mapping in Bangladesh Using Standardized Precipitation Index during 1981–2010. *Adv. Meteorol.* **2017**, *2017*, 4642060. [[CrossRef](#)]
48. Murad, H.; Islam, A.S. Drought assessment using remote sensing and GIS in north-west region of Bangladesh. In Proceedings of the 3rd International Conference on Water & Flood Management, Dhaka, Bangladesh, 8–10 January 2011; pp. 797–804.
49. Rafiuddin, M.; Dash, B.K.; Khanam, F. Diagnosis of Drought in Bangladesh using Standardized Precipitation Index. In *Proceedings of the International Conference on Environment Science and Engineering*; IACSIT Press: Singapore, 2011.
50. Shahid, S.; Behrawan, H. Drought risk assessment in the western part of Bangladesh. *Nat. Hazards* **2008**, *46*, 391–413. [[CrossRef](#)]
51. Rahman, A.A.; Alam, M.; Alam, S.S.; Uzzaman, M.R.; Rashid, M.; Rabbani, G. *Risks, Vulnerability, and Adaptation in Bangladesh*; UNDP Human Development Report, Bangladesh Centre for Advanced Studies (BCAS): Dhaka, Bangladesh, 2008.
52. Paul, B.K. Coping mechanisms practiced by drought victims (1994/95) in North Bengal, Bangladesh. *Appl. Geogr.* **1998**, *18*, 355–373. [[CrossRef](#)]
53. Habiba, U.; Hassan, A.W.R.; Shaw, R. Livelihood adaptation in the drought-prone areas of Bangladesh. In *Climate Change Adaptation Actions in Bangladesh*; Springer: Tokyo, Japan, 2013; pp. 227–252. ISBN 978-4-431-54248-3.
54. Rashid, H.E. *Geography of Bangladesh*; University Press Limited: Dhaka, Bangladesh, 1991.
55. Deo, R.C.; Sahin, M. Application of the extreme learning machine algorithm for the prediction of monthly Effective Drought Index in eastern Australia. *Atmos. Res.* **2015**, *153*, 512–525. [[CrossRef](#)]

56. Morid, S.; Smakhtin, V.; Bagherzadeh, K. Drought forecasting using artificial neural networks and time series of drought indices. *Int. J. Climatol.* **2007**, *27*, 2103–2111. [[CrossRef](#)]
57. Kim, D.W.; Byun, H.R. Future pattern of Asian drought under global warming scenario. *Appl. Clim.* **2009**, *98*, 137–150. [[CrossRef](#)]
58. Cho, J.; Cho, W.; Jung, I. RSQM: Statistical Downscaling Toolkit for Climate Change Scenario Using Nonparametric Quantile Mapping. 2018. Available online: cran.r-project.org/web/packages/rSQM/index.html (accessed on 24 May 2018).
59. Gudmundsson, L.; Bremnes, J.B.; Haugen, J.E.; Engen-Skaugen, T. Technical Note: Downscaling RCM precipitation to the station scale using statistical transformations—A comparison of methods. *Hydrol. Earth Syst. Sci.* **2012**, *16*, 3383–3390. [[CrossRef](#)]
60. Fahad, M.G.R.; Saiful Islam, A.K.M.; Nazari, R.; Hasan, M.A.; Tarekul Islam, G.M.; Bala, S.K. Regional changes of precipitation and temperature over Bangladesh using bias-corrected multi-model ensemble projections considering high-emission pathways. *Int. J. Climatol.* **2007**, *38*, 1634–1648. [[CrossRef](#)]



© 2019 by the authors. Licensee MDPI, Basel, Switzerland. This article is an open access article distributed under the terms and conditions of the Creative Commons Attribution (CC BY) license (<http://creativecommons.org/licenses/by/4.0/>).